

## Effect of acid mine drainage on dissolved rare earth elements geochemistry along a fluvial–estuarine system: the Tinto-Odiel Estuary (S.W. Spain)

J. Borrego, B. Carro, N. López-González, J. de la Rosa, J. A. Grande, T. Gómez and M. L. de la Torre

### ABSTRACT

The concentration of rare earth elements together with Sc, Y, and U, as well as rare earth elements fractionation patterns, in the water of an affected acid mine drainage system were investigated. Significant dissolved concentrations of the studied elements were observed in the fluvial sector of this estuary system (Sc  $\sim 31 \mu\text{g L}^{-1}$ , Y  $\sim 187 \mu\text{g L}^{-1}$ , U  $\sim 41 \mu\text{g L}^{-1}$ ,  $\Sigma$  rare earth elements  $\sim 621 \mu\text{g L}^{-1}$ ), with pH values below 2.7. In the mixing zone of the estuary, concentrations are lower (Sc  $\sim 2.1 \mu\text{g L}^{-1}$ ; Y  $\sim 16.7 \mu\text{g L}^{-1}$ ; U  $\sim 4.8 \mu\text{g L}^{-1}$ ;  $\Sigma$  rare earth elements  $\sim 65.3 \mu\text{g L}^{-1}$ ) and show a strong longitudinal gradient. The largest rare earth elements removal occurs in the medium-chlorinity zone and it becomes extreme for heavy rare earth elements, as observed for Sc. Samples of the mixing zone show a North American Shale normalized pattern similar to the fluvial zone water, while the samples located in the zone with pH between 6.5 and 7.7 show a depletion of light rare earth elements relative to middle rare earth elements and heavy rare earth elements, similar to that observed in samples of the marine estuary.

**Key words** | acidic river-estuary, dissolved rare earth elements, fractionation pattern, Iberian Pyrite Belt, Spain

J. Borrego  
B. Carro  
N. López-González  
J. de la Rosa  
Departamento de Geología,  
Facultad de Ciencias Experimentales,  
Universidad de Huelva, Campus El Carmen,  
21071 Huelva,  
Spain

J. A. Grande (corresponding author)  
T. Gómez  
M. L. de la Torre  
Grupo Geología Costera y Recursos Hídricos,  
Universidad de Huelva, Campus de la Rábida,  
Escuela Politécnica Superior,  
21819 Palos de la Frontera, Huelva,  
Spain  
E-mail: grangil@uhu.es

### INTRODUCTION

In recent times, many studies on the composition of rare earth elements (REEs) in water, suspended matter, and sediments of rivers and estuaries have been performed (Elderfield *et al.* 1990; Sholkovitz 1992; Zhu *et al.* 1997; Singh & Rajamani 2001; Lawrence & Kamber 2006). Some of these studies focused on the REE behaviour in adverse environmental conditions, explaining the different REE fractionation patterns. The properties of these elements, combined with their sensitivity to changes in pH, redox conditions, and adsorption/desorption reactions, allow their use as indicators of input provenance and weathering processes, or as tracers of changes in the environmental conditions in the water systems (Sholkovitz 1992; Leybourne *et al.* 2000; Åström 2001). Moreover, they can be a relevant tool for determining the effects of anthropogenic activities, like the

discharge of solid or liquid effluents, on natural environments that modify their geochemical characteristics. The use of REEs as natural tracers requires knowing the factors that control the fractionation patterns of these elements. One of the environmental indicators used is the Ce anomaly, because Ce is an element very sensitive to changes in redox conditions. In surface waters, and especially in marshlands, this element shows a strong negative anomaly produced by oxidation of  $\text{Ce}^{3+}$  to  $\text{Ce}^{4+}$  and the preferential removal of  $\text{Ce}^{4+}$ . In reducing conditions, oxidation of  $\text{Ce}^{3+}$  is inhibited, which gives rise to positive Ce anomalies (Leybourne *et al.* 2000).

Fluvial waters are characterized by a light REE (LREE) depleted pattern, with respect to middle REE (MREE) and high REE (HREE), as a result of the combination of their

aquatic chemistry and weathering processes (Byrne & Sholkovitz 1996). This depletion continues when rivers reach estuaries, where an LREE preferential removal (modification of REE concentrations longitudinally in estuaries) occurs in low salinity mixing zones (Sholkovitz 1995). An extensive revision of the behaviour of the REE in estuaries can be seen in Lawrence & Kamber (2006).

One of the most important alterations affecting the geochemistry of REE and other trace elements is acid mine drainage (AMD) processes (Elbaz-Poulichet & Dupuy 1999; Protano & Riccobono 2002; Bozau *et al.* 2004; Olias *et al.* 2005). AMD is one of the most widespread environmental problems worldwide and is mainly generated by the mining of coal and polymetallic sulphide deposits. Oxidation of pyrite (FeS<sub>2</sub>) by exposure to atmospheric O<sub>2</sub> during or after mining operations generates acidic waters with high sulphate, Fe, and heavy metal concentrations. From the environmental point of view, much attention has been paid to the danger of heavy metals associated with AMD processes (Hg, As, Pb, and Cd, among others) (Sáinz *et al.* 2004; Olias *et al.* 2005). Another effect is the increase in REE (lanthanide series) concentration in both the water and sediments affected by AMD processes (Elbaz-Poulichet & Dupuy 1999; Protano & Riccobono 2002; Bozau *et al.* 2004; Olias *et al.* 2005).

The aim of the present work was to describe the content, behaviour, and fractionation pattern of REEs and some trace elements (Sc, Y, and U), which are present in the dissolved phases of the water along a river–estuarine system affected by AMD and with a high heavy metal concentration.

## REGIONAL SETTING

The Tinto and Odiel Rivers are located in the SW of Spain. Both rivers are located in a climatic zone of extremely irregular rainfall. Their hydrological behaviour is very different in the wet and dry seasons (Sáinz *et al.* 2004).

The Tinto River is nearly 100 km long and has a drainage basin of 720 km<sup>2</sup>, associated with a clearly seasonal flow regime, with mean annual values of 2.85 m<sup>3</sup>s<sup>-1</sup> and with minimum values in the summer, of approximately 0.1 m<sup>3</sup>s<sup>-1</sup> (Borrego 1992). The Tinto River drainage basin

crosses through materials belonging to the most southern units of the Hesperian Massif in the Iberian Peninsula, occupying a large part of the so-called Central Domain or Iberian Pyrite Belt (Figure 1), which is the largest repository of volcanogenic massive sulphide deposits in the world. The massive sulphide deposits of the Riotinto mining district are the biggest in the world and contain over 10<sup>9</sup> tons of massive pyrite ore. These deposits have abundant base metal sulphides (Zn, Cu, Pb) and associated trace metals (Cd, As, Tl, Sn, Hg, Ag, and Au). These give the sector characteristics that favour AMD processes and make the Tinto River a system characterized by pH lower than 3, and high dissolved metal concentrations (Elbaz-Poulichet *et al.* 1999; Davis *et al.* 2000; Elbaz-Poulichet *et al.* 2000; Grande *et al.* 2000; Borrego *et al.* 2002).

The Tinto River flows into the Atlantic Ocean forming a common estuary with the Odiel River, known as The Ria of Huelva (Figure 1). This estuarine system is affected by a semidiurnal mesotidal regime, with a mean tidal range of 2.69 to 3.06 m range during spring tides and a 1.70 m range, during neap tides. The Tinto River contributions to the estuary are seasonal and highly variable from year to year. Mean discharge is 3.2 m<sup>3</sup>s<sup>-1</sup>, but it may exceed 21.2 m<sup>3</sup>s<sup>-1</sup> in the most rainy months. Conversely, discharge is very low (flows <0.5 m<sup>3</sup>s<sup>-1</sup>) during the dry summer months (Carro 2002; López-González 2002).

Since 1966, fertilizer factories, copper foundries, paper mills, as well as phosphogypsum deposits and plants for cleaning aggregates have been established along the lower course of the Tinto River. This industrial activity generates a large volume of effluents that find their way into the waters of the estuary and contribute large quantities of heavy metals and nutrients, making this one of the most polluted estuarine systems in Western Europe (Ruiz *et al.* 1998; Grande *et al.* 2000; Borrego *et al.* 2002). In the fertilizer factories, phosphoric acid is obtained through the chemical treatment of phosphate rock. Additionally, in this chemical process, a byproduct called phosphogypsum is formed. Phosphogypsum is mainly composed of gypsum (CaSO<sub>4</sub>·2H<sub>2</sub>O) but also contains minor quantities of fluoride, trace and REE (Arocena *et al.* 1995). Phosphogypsum stacks cover about 12 km<sup>2</sup> of the salt marshes located in the left margin of the Tinto estuary (Figure 1) and generate a high radioactive impact on this marshland (Bolívar *et al.* 2002).

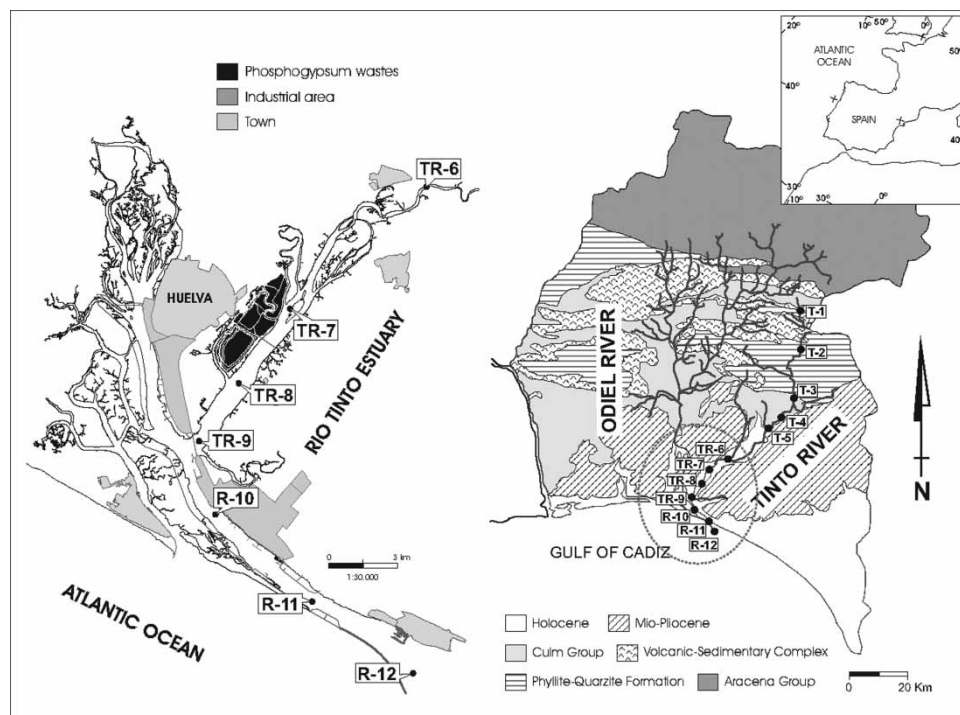


Figure 1 | Location of water sampling sites in the Tinto river-estuary.

together with large amounts of P, As, U, Th, and  $^{226}\text{Ra}$  (Elbaz-Poulichet *et al.* 2000; Alcaraz Pelegrina & Martínez-Aguirre 2007).

## MATERIALS AND METHODS

In the summer of 2002, 12 surface water samples were taken from the main course of the Tinto River (Figure 1). The pH and electrical conductivity were determined in the field. The water samples were collected in 500-ml polyethylene bottles and filtered through a 0.2- $\mu\text{m}$  Millipore Teflon filter and kept cold. From the filtered water, two subsamples were obtained. Subsamples for cation analysis were acidified with  $\text{HNO}_3$  Suprapur<sup>®</sup> Merck to pH lower than 2. The concentration of ionic Cl in the filtered water samples was determined in an ionic chromatograph for water samples, made up of an isocratic pump, a conductivity detector, and high-capacity separating columns for the quantitative detection of inorganic anions.

The analyses were performed in the laboratories of the R&D Central Services of the University of Huelva. The

ICP-MS (HP4500) technique was used to determine  $^{45}\text{Sc}$ ,  $^{89}\text{Y}$ ,  $^{139}\text{La}$ ,  $^{140}\text{Ce}$ ,  $^{141}\text{Pr}$ ,  $^{146}\text{Nd}$ ,  $^{147}\text{Sm}$ ,  $^{153}\text{Eu}$ ,  $^{157}\text{Gd}$ ,  $^{159}\text{Tb}$ ,  $^{163}\text{Dy}$ ,  $^{165}\text{Ho}$ ,  $^{166}\text{Er}$ ,  $^{172}\text{Yb}$ ,  $^{175}\text{Lu}$ , and  $^{232}\text{Th}$ . The ICP-MS operating conditions were used in this work. The instrument was optimized using solutions of 10 ppb of  $^7\text{Li}$ ,  $^{89}\text{Y}$ , and  $^{205}\text{Tl}$ . The maximum sensitivity obtained was 15,000 cps for  $^7\text{Li}$ , 55,000 cps for  $^{89}\text{Y}$ , and 41,000 cps for  $^{205}\text{Tl}$ .

An external calibration was used, with multi-elemental solutions SPEX 1 (REE) and SPEX 2 (alkaline, alkaline earths, and metals) as blank, 1  $\mu\text{g/L}$ , 10  $\mu\text{g/L}$ , and 50  $\mu\text{g/L}$ . During the analysis sequence, the instrument drift was controlled by a multi-elemental solution of 10  $\mu\text{g/L}$ , which was included periodically among the samples (every eight samples) to monitor signal change during the performance of the sequence. The measurement precision was greater than 5% RSD (relative standard deviation) for all REEs and most of the other elements analysed by repeated analysis of a multi-elemental solution of 10  $\mu\text{g/L}$ . The detection limit was close to 0.01  $\mu\text{g/L}$  for all determinations. In this sector, North American Shale Composite (NASC) normalized patterns show a convex-up pattern centred on Gd.

## RESULTS

The mean values of pH, conductivity, chlorinity, and contents of Sc, U, Y, and REE of the samples are listed in Table 1. To avoid complication in the variation of REE absolute concentrations due to natural abundance, normalization to the REE values in North American Shale Composite (NASC) (Taylor & McLennan 1985) is currently used in the field of marine geochemistry. Table 2 shows the concentrations of total rare earth elements ( $\Sigma\text{REE}$ ), light REE (LREE: La to Eu), heavy REE (HREE: Gd to Lu), Ce-anomalies ( $\text{Ce}^* = \text{Ce}/(\text{La} \times \text{Pr})^{1/2}$ ), and normalized concentration ratios of (La/Gd), (La/Yb) of the analysed samples and the mean values for river and ocean waters (Taylor & McLennan 1985). (La/Gd), (La/Yb) ratios show concentration variations between the groups of LREE represented by La and middle REE (MREE) represented by Gd, and the group of HREE represented by Yb.

In the fluvial sector, pH remains almost constant, with values ranging from 2.57 to 2.65 (Table 1, Figure 2). In the upper zone of this sector, samples show the highest conductivity (between 17.31 and 15.84  $\text{mS cm}^{-1}$ ) and lowest chlorinity ( $<0.04 \text{ g L}^{-1}$ ). In the mixing zone of the estuary, located between the limit of the tidal influence and the confluence of the Tinto and Odriel rivers (Figure 1), pH increases from 2.73 to 7.92 along this reach of the Tinto River (samples TR-6 to TR-9). In the marine estuary, pH, conductivity, and chlorinity values remain constant (Figure 2).

## DISCUSSION

### Characteristics of water (pH, conductivity, and chlorinity)

The samples of the upper zone of the fluvial sector are directly affected by acid drainage from the mines located at the source of the Tinto River and show high concentration of dissolved sulphate (Sáinz *et al.* 2004). Conductivity values decrease downstream, oscillating between 5.40 and 4.20  $\text{mS cm}^{-1}$  (Table 1, Figure 2). This decrease is due to the formation of secondary oxide, oxyhydroxysulphates, and sulphates in alluvium downstream of the mining areas. The soluble Fe oxyhydroxysulphates

such as copiapite are a store of metal and REE (Hudson-Edwards *et al.* 1999; Elbaz-Poulichet & Dupuy 1999).

The strong gradient in pH values in the mixing zone of the estuary is caused by the mixing of river water ( $\text{pH} < 3$ ) with the slightly basic seawater ( $\text{pH}$  between 7.9 and 8.3). The same process causes a strong longitudinal gradient in conductivity and chlorinity, which range from 4.70 (sample TR-6) to 143.20  $\text{mS cm}^{-1}$  (sample TR-9) and 1.39 to 16.4  $\text{g L}^{-1}$ , respectively.

In the marine estuary pH varies from 7.94 to 7.99, conductivity between 138.20 and 142.10  $\text{mS cm}^{-1}$  and chlorinity from 18.1 to 19.8  $\text{g L}^{-1}$ . Marine conditions prevail in this sector and only during high river discharge, pH values are lower than 7 and conductivity does not exceed 120  $\text{mS cm}^{-1}$  (Borrego 1992).

### Distribution and concentrations of Sc, U, and Y

Sc concentration varies between 50.81 and 11.43  $\mu\text{g L}^{-1}$ , U between 76.7 and 12.2  $\mu\text{g L}^{-1}$ , and Y between 363.10 and 55.19  $\mu\text{g L}^{-1}$ . These concentrations are several orders of magnitude higher than mean concentrations of these elements in river waters (Taylor & McLennan 1985) and very similar to those present in other water systems affected by acid drainage (Gammons *et al.* 2003). In all cases, the concentration of these elements decreases downstream, in direct relation to conductivity reduction (Figure 2). This is due to the formation of oxyhydroxysulphates and sulphates in alluvium downstream of the mining areas, which are a temporary store of metals (Hudson-Edwards *et al.* 1999).

In the estuarine mixing zone, dissolved trace element concentrations are significantly lower than those in the fluvial sector. Sc ranges from 6.30 to 0.13  $\mu\text{g L}^{-1}$ , U from 7 to 2.7  $\mu\text{g L}^{-1}$ , and Y from 45.88 to 0.15  $\mu\text{g L}^{-1}$  (Table 1). The longitudinal gradient presented by these element concentrations in the estuarine mixing zone is stronger than that in the fluvial sector (Figure 2). This is because in estuaries, the behaviour of dissolved trace elements is mainly controlled by water-particle interactions and solution chemistry, i.e., flocculation, organic and inorganic complexation, adsorption, and sediment re-suspension (Sholkovitz 1976, 1978). In most estuarine systems, these processes originate by mixing between fresh and salt water. However, in the Tinto River estuary, another phenomenon is added:

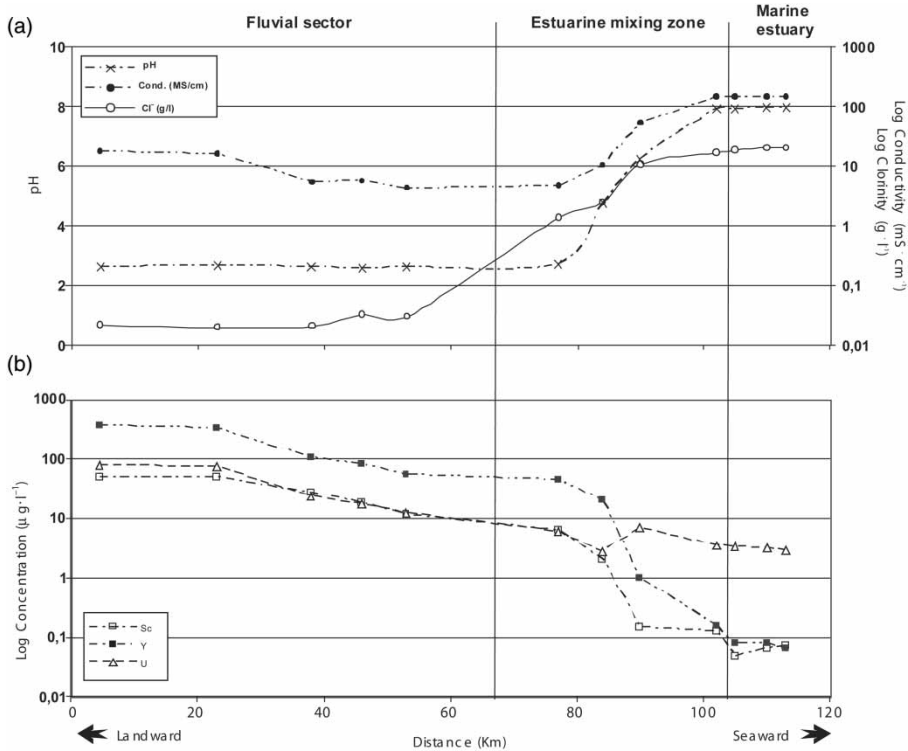
**Table 1** | pH, electrical conductivity (mS cm<sup>-1</sup>) and chlorinity (g L<sup>-1</sup>), Sc, U, Y and REE contents (μg L<sup>-1</sup>) of the Tinto river–estuary samples

Samples	Fluvial sector					Mean	Estuarine mixing zone					Mean	Marine estuary			Mean
	T-1	T-2	T-3	T-4	T-5		TR-6	TR-7	TR-8	TR-9	R-10		R-11	R-12		
pH	2.62	2.65	2.64	2.57	2.64	2.62	2.73	4.75	6.22	7.92	5.41	7.94	7.99	7.99	7.97	
Cond (mS cm <sup>-1</sup> )	17.31	15.84	5.40	5.46	4.20	9.64	4.70	10.20	51.70	143.20	52.45	138.20	141.30	142.10	140.53	
Cl* (gr L <sup>-1</sup> )	0.22	0.20	0.21	0.26	0.30	0.24	1.39	2.48	10.40	16.40	7.67	18.49	19.62	19.85	19.32	
Concentration (μg L <sup>-1</sup> )																
Sc	50.81	48.72	27.30	18.42	11.43	31.34	6.30	1.99	0.15	0.13	2.14	0.05	0.06	0.07	0.06	
Y	365.10	333.44	104.84	81.63	55.19	187.64	45.88	19.70	1.00	0.15	16.68	0.08	0.08	0.06	0.07	
U	76.72	73.06	22.88	17.40	12.24	40.46	6.00	2.73	7.06	3.48	4.82	3.34	3.12	2.91	3.12	
La	84.46	85.47	40.46	30.44	21.55	52.48	24.49	10.44	0.62	0.08	8.91	0.04	0.03	0.02	0.03	
Ce	378.28	377.37	151.69	83.65	60.34	210.27	56.95	30.68	1.24	0.15	22.25	0.04	0.02	0.02	0.03	
Pr	48.25	47.81	19.25	14.00	9.54	27.77	9.12	3.80	0.12	0.04	3.27	0.01	0.02	0.01	0.01	
Nd	231.98	229.11	89.85	66.93	45.28	132.63	36.44	17.41	0.58	0.14	13.64	0.04	0.05	0.05	0.05	
Sm	73.92	72.07	26.52	19.51	12.93	40.99	9.79	4.56	0.12	0.09	3.64	0.05	0.06	0.05	0.05	
Eu	17.56	17.27	6.07	4.47	3.00	9.67	2.16	0.97	0.03	0.04	0.80	0.03	0.03	0.02	0.03	
Gd	86.48	85.71	30.93	23.40	15.76	48.46	11.81	5.69	0.19	0.12	4.45	0.04	0.07	0.04	0.05	
Tb	13.50	13.35	4.75	3.61	2.39	7.52	1.55	0.83	0.02	0.02	0.60	0.01	0.01	0.01	0.01	
Dy	74.42	74.08	26.17	19.99	13.41	41.61	10.04	4.62	0.19	0.08	3.73	0.06	0.06	0.05	0.05	
Ho	14.74	14.66	5.10	3.92	2.62	8.21	1.58	0.82	0.02	0.03	0.61	0.01	0.01	0.02	0.01	
Er	38.44	38.25	13.23	10.12	6.81	21.37	4.95	2.20	0.07	0.02	1.81	0.01	0.02	0.01	0.01	
Yb	31.81	31.49	10.76	8.22	5.47	17.55	3.74	1.64	0.03	0.05	1.36	0.03	0.03	0.03	0.03	
Lu	4.80	4.70	1.62	1.23	0.81	2.63	0.53	0.24	0.01	0.02	0.20	0.01	0.01	0.00	0.01	

**Table 2** | Total REE ( $\Sigma$ REE), light REE and heavy REE ( $\mu\text{g L}^{-1}$ ), and (La/Gd), (La/Yb) and Ce\* anomaly of the Tinto river–estuary water

	Samples	$\Sigma$ REE	LREE	HREE	(La,Gd) <sub>NASC</sub>	(La/Yb) <sub>NASC</sub>	Ce*
Fluvial sector	T-1	1098.63	816.89	281.74	0.16	0.26	1.29
	T-2	1091.35	811.84	279.52	0.16	0.26	1.29
	T-3	426.38	327.78	98.61	0.21	0.36	1.18
	T-4	289.48	214.52	74.95	0.21	0.36	0.88
	T-5	199.92	149.65	50.27	0.22	0.38	0.92
	Mean	621.15	464.14	157.02	0.19	0.32	1.11
Estuarine mixing zone	TR-6	173.12	136.78	36.34	0.34	0.63	0.83
	TR-7	83.91	66.89	17.02	0.30	0.62	1.06
	TR-8	3.22	2.68	0.55	0.55	2.19	1.01
	TR-9	0.88	0.51	0.37	0.12	0.17	0.58
	Mean	65.28	51.71	13.57	0.32	0.90	0.87
Marine estuary	R-10	0.37	0.17	0.20	0.17	0.15	0.35
	R-11	0.43	0.19	0.24	0.07	0.11	0.22
	R-12	0.33	0.15	0.18	0.09	0.08	0.24
	Mean	0.38	0.17	0.21	0.11	0.11	0.27
River water*		0.20	0.18	0.03	0.92	1.29	0.92
Ocean water*		0.02	0.01	0.00	0.73	0.48	0.36

\* Taylor &amp; McLennan 1985

**Figure 2** | Diagrams of (a) pH-electrical conductivity and chlorinity (b) Sc, Y and U concentrations ( $\mu\text{g L}^{-1}$ ) versus the distance from the source of the Tinto River.

the effect of the acid mixing and the effluents generated by the industry located near the estuary, which represents a unique phenomenon (Borrego et al. 2004a, b).

Scandium and Y concentration decreases in constant form with increasing conductivity and chlorinity, both elements showing a non-conservative behaviour in the

estuarine mixing zone (Figure 2). In the case of Sc, the reduction is sharper in the low-medium chlorinity zone (between 2.3 and 10.4 g L<sup>-1</sup>), going from a concentration of 6.30 to 0.15 µg L<sup>-1</sup> (Figure 3). Yttrium concentration shows a continuous decline along the whole mixing zone (with chlorinity values from 2.3 to 16.4 g L<sup>-1</sup>), going from 45.88 to 0.15 µg L<sup>-1</sup>. This indicates that Sc removal occurs faster than Y removal, because Sc has a smaller ionic radius and is quickly hydrolyzed, showing a hydrogeochemical behaviour similar to Fe<sup>3+</sup> (Brookins 1989). Thus, the rapid increase of pH (from 2.73 to 4.75) in the low-medium chlorinity zone accelerates dissolved Sc removal and its adsorption by suspended particles.

In the case of U, extreme removal takes place at very low chlorinity levels (lower than 2.3 g L<sup>-1</sup>) and pH below 5 (Figure 2). Under these conditions, dissolved U concentration

goes from 6 to 1.9 µg L<sup>-1</sup>. In the medium-high chlorinity zone (between 10.4 and 16.4 g L<sup>-1</sup>), U concentration varies from 2.7 (TR-8) to 7.1 (TR-9) µg L<sup>-1</sup>; probably because this zone is affected by runoff coming from the phosphogypsum deposits located on the left bank of the estuary (Figure 1). In the marine zone, concentrations of these three elements (Sc, U, and Y) do not show significant variations, remaining approximately constant (Table 1, Figure 2).

### Concentration of REE, (La/Gd), and (La/Yb) ratios and NASC-normalized patterns

For samples located in the fluvial sector, REE concentrations are similar to those observed in other water systems affected by acid drainage (Protano & Riccobono 2002) and very high compared with unaffected river systems. Thus, total REE

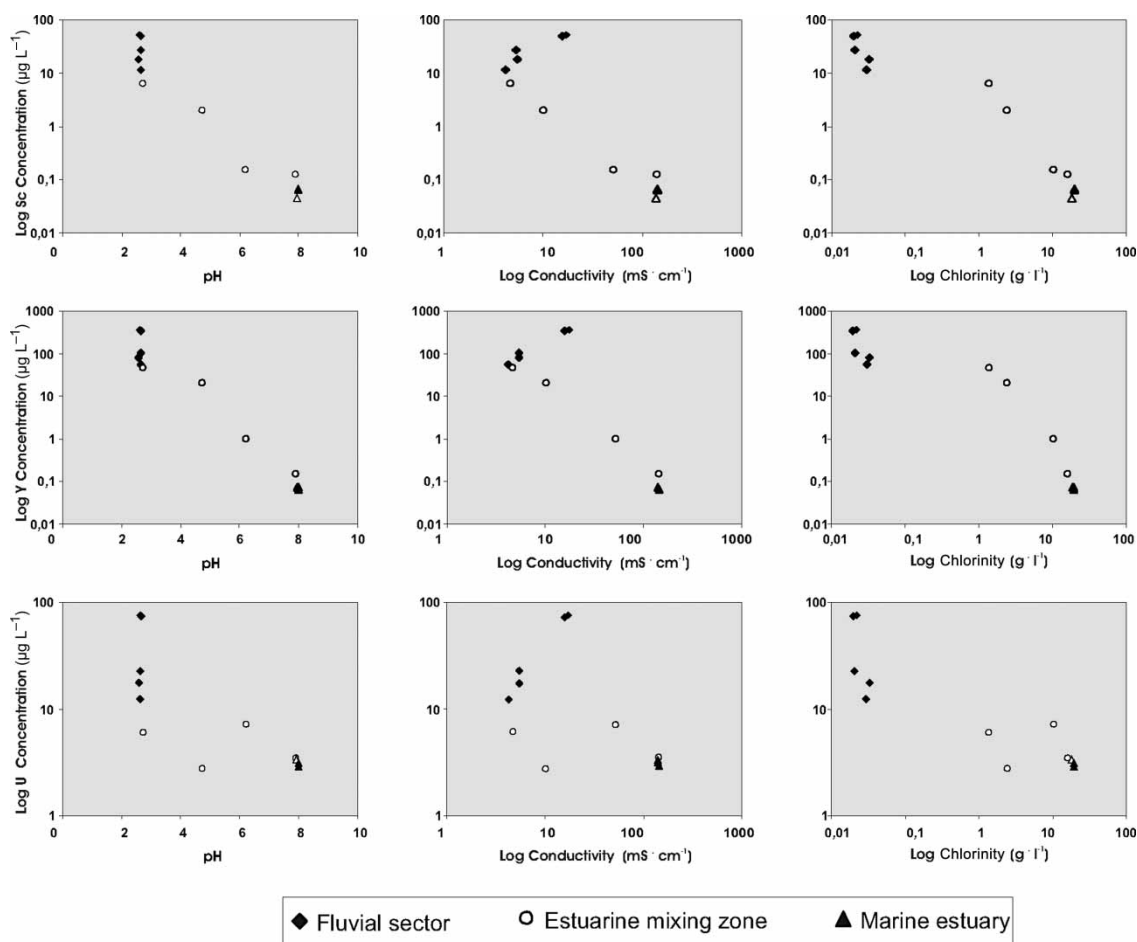
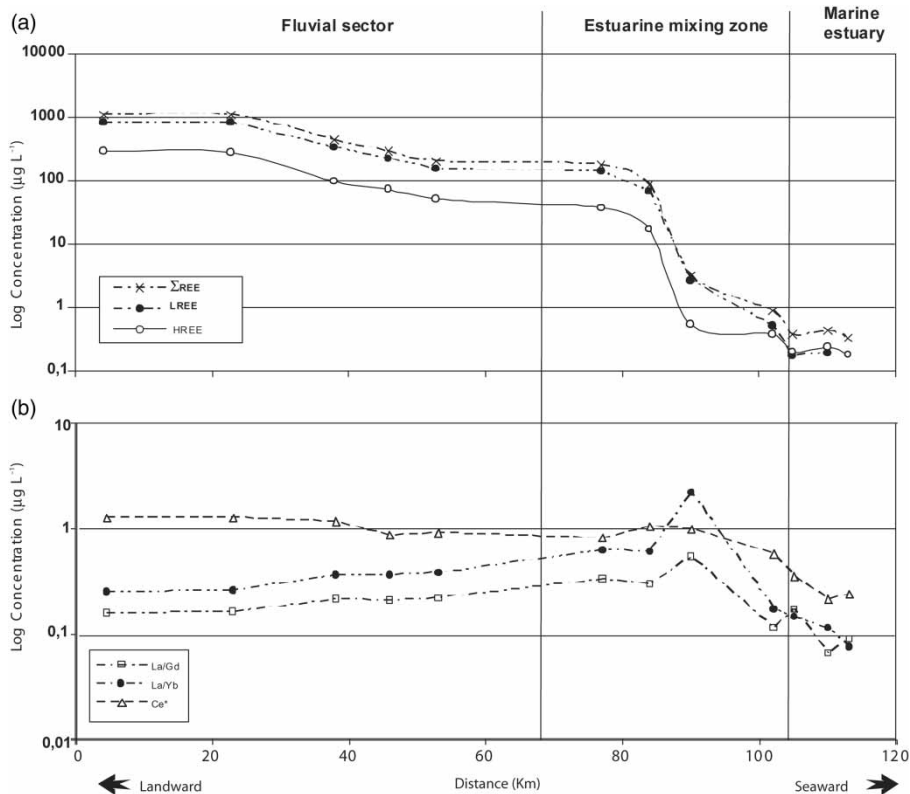


Figure 3 | Plots of Sc, Y and U (µg L<sup>-1</sup>) versus pH, electrical conductivity (mS cm<sup>-1</sup>) and chlorinity (g L<sup>-1</sup>).

( $\Sigma$ REE) concentration ranges from 1,098.63 to 199.92  $\mu\text{g L}^{-1}$ , in contrast to mean river water concentration (0.20  $\mu\text{g L}^{-1}$ , by Taylor & McLennan 1985). REE contents decrease downstream, in direct relation with the conductivity decrease (Figure 4). Conversely, (La/Gd) and (La/Yb) ratios show a slight increase downstream (Figure 4), which is evidence for a relative increase in LREE concentration as opposed to MREE and HREE. The samples of the river sector with the highest conductivity values are located in proximity of the mining operations (samples T-1 to T-3) and show a slight positive Ce\* anomaly, which ranges from 1.18 to 1.29 (Table 2, Figure 4). Further downstream (samples T-4 and T-5), the Ce\* anomaly decreases to slightly less than 1, matching the lowest conductivity values (Table 1). The REE decrease downstream of the mining areas may be due to the sulphate precipitation at the alluvial deposits of the river, so the REE-SO<sub>4</sub> complexes are the dominant species (Elbaz-Poulichet & Dupuy 1999) in the SO<sub>4</sub>-rich water.

In the fluvial zone, the NASC-normalized patterns (Figure 5) are dominated by distinct convexity centred on

Gd, which reflects an enrichment of MREE over both LREE and HREE. The same pattern has been observed in other water systems affected by acid drainage (Johannesson & Lyons 1995; Protano & Riccobono 2002). Several mechanisms are mainly thought to be responsible for MREE enrichment, such as dissolution or leaching of MREE-enriched minerals, amorphous phases, or mineral surface coatings (Gosselin *et al.* 1992; Johannesson & Zhou 1999), and fractionation by colloid-borne REE (Elderfield *et al.* 1990). Middle REE-enriched patterns are typical of other water systems, not only for acidic environments (Bozau *et al.* 2004). The origin of this enrichment is not clearly known at present, although in the Tinto River case it may be caused by preferential dissolution, under acidic conditions, of Fe hydroxides and oxyhydroxides (Gimeno *et al.* 1996; Johannesson *et al.* 1996). Iron hydroxides and oxyhydroxides such as goethite and ferrihydrite occur in cements in both the mining areas and alluvium downstream. Dissolution of these minerals in the upper zones of the Tinto River would cause high concentrations of sulphate, Fe, and



**Figure 4** | Diagrams of (a) total REE ( $\Sigma$ REE), LREE and HREE ( $\mu\text{g L}^{-1}$ ) and (b) La/Gd, La/Yb and Ce\* anomaly versus the distance from the source of the Tinto River.

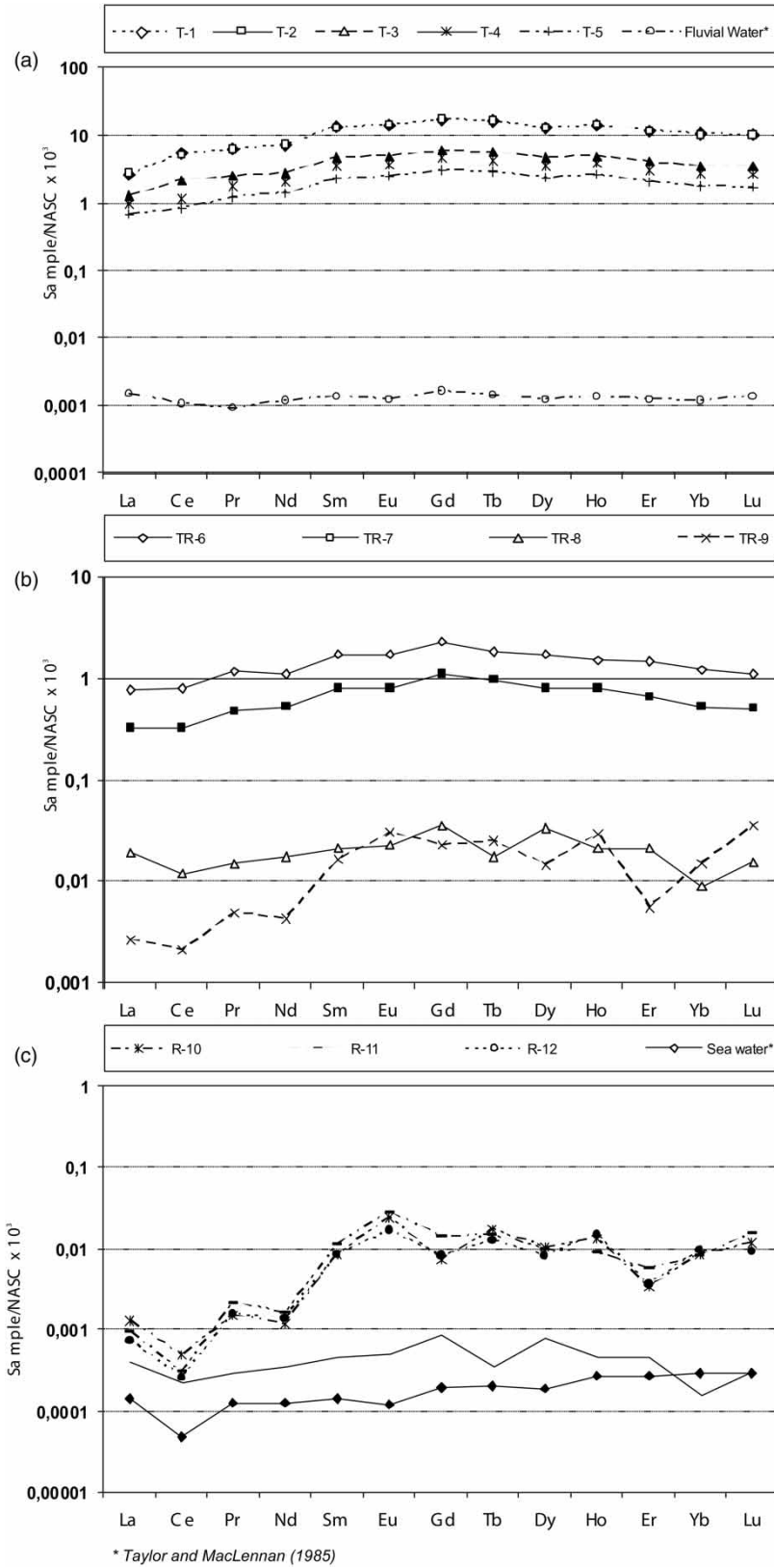


Figure 5 | NASC-normalized REE profiles for waters collected in the Tinto system: (a) the fluvial sector; (b) the estuarine mixing zone; (c) the marine estuary.

heavy metals in the water (Hudson-Edwards *et al.* 1999), possibly giving rise to MREE enrichment.

In the estuarine mixing zone, total REE ( $\Sigma$ REE) concentration decreases continually with increasing conductivity and chlorinity, showing a non-conservative behaviour in the estuarine mixing zone (Figure 2) and strong longitudinal gradient (Table 2, Figure 4). Samples with low pH (<3) located at the limit of the fluvial sector (like TR-6) show high concentrations ( $173.12 \mu\text{g L}^{-1}$ ), while in the confluence with the marine sector (TR-9), concentration is very low ( $<1 \mu\text{g L}^{-1}$ ). The highest REE removal occurs in the medium chlorinity zone (between  $1.5$  and  $10.4 \text{ g L}^{-1}$ ) with pH values between 4 and 6 (Figure 5). Removal is not the same for the whole REE group, being more extreme for HREE, going from  $17.02$  to  $0.55 \mu\text{g L}^{-1}$ . This REE removal is similar to that observed in Sc, because the ionic radius decreases from LREE to HREE, making the behaviour of the latter closer to Sc. The same effect has been observed in other water environments affected by AMD (Olias *et al.* 2005).

A similar effect is observed in (La/Gd) and (La/Yb) ratios (Figure 4), which increase with pH between 2.73 and 6.22 in the low-medium chlorinity zone. This reflects a relative enrichment of LREE over MREE and HREE. The REE behaviour is opposite to that observed in the mixing zones of estuaries unaffected by acid drainages, where a great REE depletion in the low salinity occur associated with formation of colloids of iron-organic matter colloids (Hoyle *et al.* 1984), or coagulation of iron oxide-organic colloids (Sholkovitz 1995). In all cases, the LREE removal is more effective than MREE and HREE (Hoyle *et al.* 1984; Elderfield *et al.* 1990; Sholkovitz 1995; Lawrence & Kamber 2006). In these cases, the salt-induced processes are dominant, while in the estuarine mixing zone of the Tinto River are the acid neutralization processes. In water systems with low pH, LREE tend to remain in the dissolved phases, while HREE and, to a lower extent, MREE are adsorbed on particle surfaces (Åström 2001). Besides, the REE removal in the estuary is related with scavenging processes of Fe oxyhydroxide precipitation, typical of salt-induced estuaries (fresh water mixed by salty water), because of redox conditions upstream of the mixing zone (water with low pH, 2–4, is mixed by a water with pH neutral or lightly alkaline, 7–8.2. (Elbaz-Poulichet & Dupuy 1999).

An extreme LREE enrichment is observed in sample TR-8, with respect to the whole system, where (La/Gd)

and (La/Yb) ratios reach the highest values, 0.55 and 2.19, respectively (Table 2, Figure 4). The situation of this sample coincides with the location of the phosphogypsum deposits (Figure 1); also with an increase of dissolved U concentration (Figure 2). The positive correlation between U with LREE and MREE is consistent with that observed in phosphatic minerals of biogenic, authigenic, and diagenetic origins, where a significant enrichment in LREE (Aly & Mohammed 1999) and MREE (Hannigan & Sholkovitz 2001) can be noted. This indicates that the surface leachates of these deposits are responsible for this anomalous LREE and U enrichment. Similar behaviours have been described in the sediments of this estuarine system associated with direct discharges of phosphogypsum into the estuary during the 1970s and 1980s period (Borrego *et al.* 2004b).

The Ce\* anomaly in the estuarine mixing zone (Figure 4) shows negative gradient from 0.83 (sample TR-6) in the upper zone, with a greater river influence, to 0.58 (sample TR-9) in the confluence with the marine sector (Table 2). This indicates an increase in the oxidizing conditions, typical for seawaters, and characterized by Ce depletion (Fleet 1984; Brookins 1989).

Within the estuarine mixing zone, the samples located closer to the fluvial sector show a similar fractionation pattern to that observed in the acid river water, with a convex-up shape centred on Gd. Conversely, the sample located near the confluence with the sea sector shows a clearly different pattern, with LREE depletion relative to MREE and HREE (Figure 6). This indicates a rapid LREE removal when chlorinity values over  $10 \text{ g L}^{-1}$  and pH greater than 6 are reached. This is consistent with what is described by other authors for water systems unaffected by acidic mixing, where preferential removal of LREE relative to the rest of REE occurs. Thus, LREE are adsorbed on the particle surfaces present in the suspended matter, while the rest of REE remain dissolved (Sholkovitz 1992; Nozaki *et al.* 2000).

Samples within the marine sector of the estuary show the lowest REE concentrations in the whole system, ranging from  $0.33$  to  $0.43 \mu\text{g L}^{-1}$  (Table 2). However, these concentrations are much higher than mean concentration observed in the seawater ( $0.02 \mu\text{g L}^{-1}$ , by Taylor & McLennan 1985). This is more notable in HREE, which shows a concentration 40 times higher than ocean water ( $0.20 \mu\text{g L}^{-1}$

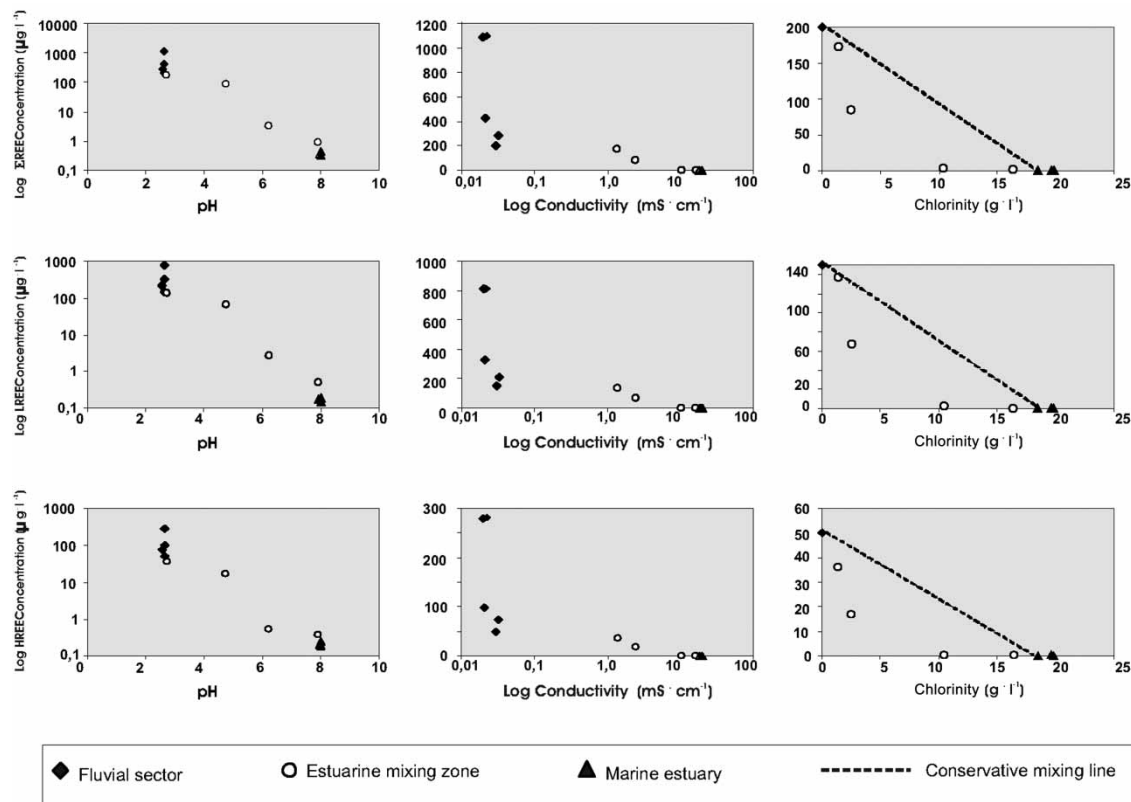


**Figure 6** | Plots of  $\Sigma\text{REE}$  ( $\mu\text{g L}^{-1}$ ), La/Gd, La/Yb and Ce\* anomaly versus pH, electrical conductivity ( $\text{mS cm}^{-1}$ ) and chlorinity ( $\text{g L}^{-1}$ ) for waters collected in the Tinto system.

as opposed to  $0.005 \mu\text{g L}^{-1}$ ) (Taylor & McLennan 1985). Besides, all samples of this sector show a significant negative Ce anomaly, typical for well-oxygenated sea environments, caused by continuous oxidation of  $\text{Ce}^{3+}$  to  $\text{Ce}^{4+}$  (Leybourne *et al.* 2000; Nozaki *et al.* 2000).

Fractionation patterns in the Tinto marine estuary show a clear MREE and HREE enrichment over LREE. Compared with the seawater NASC-normalized pattern, a more marked enrichment in MREE and, to a lesser extent, in HREE can be observed (Figure 6). This indicates that MREE contributed by the Tinto River acidic waters remain dissolved even under typical sea environment conditions, with high salinity and pH above 7.5. This reveals that AMD processes, which take place in the upper stretch of the Tinto River, affect the marine sector water even under low river input conditions (Carro 2002). River discharge during the sampling was only  $0.14 \text{ m}^3 \text{ s}^{-1}$ . Moreover, it also indicates that this system, together with the Odiel River estuary, can be an important source of REE and other metals to the Gulf

of Cadiz waters, as has been observed in previous works (van Geen *et al.* 1997; Elbaz-Poulichet & Dupuy 1999).

## CONCLUSIONS

The river-estuarine system of the Tinto River is affected by AMD coming from the polymetallic sulphide mining operations in the Iberian Pyrite Belt, located at the source of the river system (Rio Tinto mining district). As a result of these processes, the water system shows very low pH (<3), high sulphate content, and both high heavy metal and trace element concentrations. Low pH values remain even at the top of the estuarine mixing zone, ranging from 2.73 to 4.75. Moreover, large amounts of dissolved REE are observed along the whole system, i.e., in the fluvial sector, the estuarine mixing zone, and the marine estuary. These REE concentrations are several orders of magnitude higher than those present in similar environments

unaffected by AMD. In the mixing zone of the estuary, total REE concentration shows a strong longitudinal gradient, decreasing significantly from the low pH and conductivity zone to the high pH and conductivity sector. The greatest REE removal takes place in the zone with mean conductivity. This removal is not the same for the whole REE group, being more extreme for HREE, which present a removal similar to that observed in Sc. An extreme LREE enrichment is observed in the proximities of the phosphogypsum deposits, in agreement with a slight increase in dissolved U concentration. This indicates that surface leachate from these deposits is mainly responsible for this anomalous LREE and U enrichments. The samples of the marine estuary sector show the lowest REE concentration in the whole system, although these concentrations are higher than those present in seawaters. This phenomenon is much more remarkable in HREE.

In the fluvial sector, NASC-normalized patterns show a convex-up pattern centred on Gd, similar to other fluvial systems affected by AMD. (La/Gd) and (La/Yb) ratios also show a relative MREE enrichment related to LREE and HREE. The same behaviour is observed in the samples of the estuarine mixing zone, located in the low chlorinity sectors. In contrast, downstream, in the marine estuary, samples show a clearly different pattern with an evident LREE depletion relative to MREE and HREE. This indicates a preferential LREE removal when typical conductivity and pH values for seawater are reached. Under these conditions, LREE are adsorbed on the particle surfaces present in the suspended matter, while the rest of REE remain dissolved. Compared with seawater, these patterns indicate a marked MREE enrichment and, to a lower extent, in HREE. Thus, MREE discharged by the Tinto River acid waters remain dissolved even under conditions for typical sea environments. Besides, the results of AMD processes, which occur at the river source, affect the water of both the marine estuary and the adjacent coast.

## ACKNOWLEDGEMENTS

Financial support for this research by DGCICYT National Plan, projects REN2002-03979 and CTM2006-08298 and

Andalusia Regional Government (PAI), group RNM-276, is greatly appreciated.

## REFERENCES

- Alcaraz Peregrina, J. M. & Martínez-Aguirre, A. 2001 *Natural radioactivity in groundwaters around a fertilizer factory complex in South of Spain. Appl. Radiat. Isotopes* **55**, 419–423.
- Aly, M. M. & Mohammed, N. A. 1999 *Recovery of lanthanides from Abu Tartur phosphate rock, Egypt. Hydrometallurgy* **52**, 199–206.
- Arocena, J. M., Rutherford, P. M. & Dudas, M. J. 1995 *Heterogeneous distribution of trace elements and fluorine in phosphogypsum by-product. Sci. Total Environ.* **162**, 149–160.
- Åström, M. 2001 *Abundance and fractionation patterns of rare earth elements in streams affected by acid sulphate soils. Chem. Geol.* **175**, 249–258.
- Bolivar, J. P., García-Tenorio, R., Mas, J. L. & Vaca, F. 2002 *Radioactive impact in sediments from an estuarine system affected by industrial wastes releases. Environ. Int.* **27** (8), 639–645.
- Borrego, J. 1992 *Sedimentología del estuario del río Odiel (Huelva, S.O. España)*. PhD Thesis, University of Seville, Spain.
- Borrego, J., Morales, J. M., de la Torre, M. L. & Grande, J. A. 2002 *Geochemical characteristic of heavy metal pollution in surface sediments of the Tinto and Odiel river estuary (southwestern Spain). Environ. Geol.* **41**, 785–796.
- Borrego, J., López-González, N. & Carro, B. 2004a *Geochemical signature as paleoenvironmental markers in holocene sediments of the Tinto River Estuary (Southwestern Spain). Estuarine Coastal Shelf Sci.* **61**, 631–641.
- Borrego, J., López-González, N., Carro, B. & Lozano-Soria, O. 2004b *Origin of the anomalies in light and middle REE in sediments of an estuary affected by phosphogypsum wastes (South-Western Spain). Marine Poll. Bull.* **49**, 1045–1053.
- Bozau, E., Leblanc, M., Seidel, J. L. & Stärk, H. J. 2004 *Light rare earth elements enrichment in an acidic mine lake (Lusatia, Germany). Appl. Geochem.* **19**, 261–271.
- Brookins, D. G. 1989 *Aqueous geochemistry of rare earth elements. Rev. Mineral. Geochem.* **21** (1), 201–225.
- Byrne, R. H. & Sholkovitz, E. R. 1996 *Marine chemistry and geochemistry of the lanthanides*. In: *Handbook on the physics and chemistry of rare earths* (J. K. A. Gschneidner & L. Z. Eyring, eds.). Elsevier, New York, pp. 498–593.
- Carro, B. 2002 *Sedimentación reciente en el estuario del Río Odiel*. MSc Thesis, University of Huelva, Spain.
- Davis, R. A., Welty, A. T., Borrego, J., Morales, J. A., Pendón, J. G. & Ryan, J. G. 2000 *Rio Tinto estuary (Spain): 5000 years of pollution. Environ. Geol.* **39**, 1107–1116.
- Elbaz-Poulichet, F. & Dupuy, C. 1999 *Behaviour of rare earth elements at the freshwater-seawater interface of two acid mine rivers: the Tinto and Odiel (Andalusia, Spain). Appl. Geochem.* **14**, 1063–1072.

- Elbaz-Poulichet, F., Morley, N. H., Cruzado, A., Velasquez, Z., Achterberg, E. P. & Braungardt, C. B. 1999 Trace metal and nutrient distribution in an extremely low Ph (2.5) river-estuarine system, the Ría de Huelva (south-west Spain). *Sci. Total Environ.* **227**, 73–83.
- Elbaz-Poulichet, F., Dupuy, C., Cruzado, A., Velásquez, Z., Achterberg, E. P. & Braungardt, C. B. 2000 Influence of sorption processes by iron oxides and algae fixation on arsenic and phosphate cycle in an acidic estuary (Tinto River, Spain). *Water Resources* **34**, 3222–3230.
- Elderfield, H., Upstill-Goddard, R. & Sholkovitz, E. R. 1990 The rare earth elements in rivers, estuaries and coastal seas and their significance to the composition of ocean waters. *Geochim. Cosmochim. Acta* **54**, 971–991.
- Fleet, A. J. 1984 Aqueous and sedimentary geochemistry of rare earth elements. In: *Rare Earth Elements Geochemistry* (P. Henderson, ed.). Elsevier, Amsterdam, pp. 342–373.
- Gammons, C. H., Wood, S. A., Jonas, J. P. & Madison, J. P. 2003 Geochemistry of the rare-earth elements and uranium in the acidic Berkeley Pit lake, Butte, Montana. *Chem. Geol.* **198**, 269–288.
- Gimeno, M. J., Auqué, L. F., López-Julián, P. L., Gómez-Jiménez, J. & Mandalo, J. M. 1996 Pautas de distribución de las tierras raras en soluciones ácidas naturales. *Estud. Geol.* **52**, 11–22.
- Gosselin, D. G., Smith, M. R., Lepel, E. A. & Laul, J. C. 1992 Rare earth elements in chloride-rich ground water, Palo Duro Basin, Texas, USA. *Geochim. Cosmochim. Acta* **56**, 1495–1505.
- Grande, J. A., Borrego, J. & Morales, J. A. 2000 A study of heavy metal pollution in the Tinto-Odiel estuary in southwestern Spain using factor analysis. *Environ. Geol.* **39**, 1095–1101.
- Hannigan, R. E. & Sholkovitz, E. R. 2001 The development of middle rare earth element enrichments in freshwaters: weathering of phosphate minerals. *Chem. Geol.* **175**, 495–508.
- Hoyle, J., Elderfield, H., Gledhill, A. & Greaves, M. 1984 The behaviour of the rare earth elements during mixing of river and sea waters. *Geochim. Cosmochim. Acta* **48**, 143–149.
- Hudson-Edwards, K. A., Schell, C. & Macklin, M. 1999 Mineralogy and geochemistry of alluvium contaminated by metal mining in the Río Tinto area, southwest Spain. *Appl. Geochem.* **14**, 1015–1030.
- Johannesson, K. H. & Lyons, W. B. 1995 Rare-earth elements geochemistry of Colour Lake, an acidic freshwater lake on Axel Heiberg Island, Northwest Territories, Canada. *Chem. Geol.* **119**, 209–223.
- Johannesson, K. H., Lyons, W. B., Yelken, M. A., Gaudette, H. A. & Stezenbach, K. J. 1996 Geochemistry of rare-earth elements in hypersaline and dilute acidic natural terrestrial waters: Complexation behavior and middle rare-earth element. *Chem. Geol.* **133**, 125–144.
- Johannesson, K. H. & Zhou, X. 1999 Origin of middle earth elements enrichments in acidic water of a Canadian High Arctic lake. *Geochim. Cosmochim. Acta* **63**, 153–165.
- Lawrence, M. G. & Kamber, B. S. 2006 The behaviour of the rare earth elements during estuarine mixing – revisited. *Marine Chem.* **100**, 147–161.
- Leybourne, M. I., Goodfellow, W. D., Boyle, D. R. & Hall, G. M. 2000 Rapid development of negative Ce anomalies in surface waters and contrasting REE patterns in groundwaters associated with Zn–Pb massive sulphide deposits. *Appl. Geochem.* **15**, 695–723.
- López-González, N. 2002 *Descripción e interpretación de las facies deposicionales del sector interno en el Estuario del río Odiel*. MSc Thesis, University of Huelva, Spain.
- Nozaki, Y., Lerche, D., Sotto Alibo, D. & Snidvongs, A. 2000 The estuarine geochemistry of rare earth elements and indium in the Chao Phraya River, Thailand. *Geochim. Cosmochim. Acta* **64**, 3983–3994.
- Oliás, M., Cerón, J. C., Fernández, I. & de la Rosa, J. 2005 Distribution of rare earth elements in an alluvial aquifer affected by acid mine drainage: the Guadiamar aquifer (SW Spain). *Environ. Poll.* **135**, 53–64.
- Protano, G. & Riccobono, F. 2002 High contents of rare earth elements (REEs) in stream waters of a Cu–Pb–Zn mining area. *Environ. Poll.* **117**, 499–514.
- Ruiz, F., González-Regalado, M. L., Borrego, J., Morales, J. A., Pendón, J. G. & Muñoz, J.M. 1998 Stratigraphic sequence, elemental concentrations and heavy metal pollution in Holocene sediments from the Tinto–Odiel estuary, southwestern Spain. *Environ. Geol.* **34**, 270–278.
- Sáinz, A., Grande, J. A. & de la Torre, M. L. 2004 Characterization of heavy metal discharge into the Ria of Huelva. *Environ. Int.* **30**, 557–566.
- Sholkovitz, E. 1976 Flocculation of dissolved organic and inorganic matter during the mixing of river water and seawater. *Geochim. Cosmochim. Acta* **40**, 831–845.
- Sholkovitz, E. 1978 The flocculation of dissolved Fe, Mn, Al, Cu, Ni, Co and Cd during estuarine mixing. *Geochim. Cosmochim. Acta* **41**, 77–86.
- Sholkovitz, E. 1992 Chemical evolution of rare earths elements: fractionation between colloidal and solution phases of filtered river water. *Earth Planet. Sci. Lett.* **114**, 77–84.
- Sholkovitz, E. 1995 The aquatic chemistry of rare earth elements in rivers and estuaries. *Aquatic Geochem.* **1**, 1–34.
- Singh, P. & Rajamani, V. 2001 Geochemistry of the floodplain sediments of the Kaveri river, Southern India. *J. Sed. Res.* **71**, 50–60.
- Taylor, S. R. & McLennan, S. M. (eds.) 1985 *The Continental Crust: Its Composition and Evolution*. Blackwell, Oxford.
- Van Geen, A., Adkins, J. F., Boyle, E. A., Nelson, C. H. & Palanques, A. 1997 A 120 yr record of widespread contamination from mining of the Iberian pyrite belt. *Geology* **25**, 291–294.
- Zhu, W., Kennedy, M., de Leer, E. W. B., Zhou, H. & Alaerts, G. J. F. R. 1997 Distribution and modelling of rare earth elements in Chinese river sediments. *Sci. Total Environ.* **204**, 233–243.

First received 3 February 2010; accepted in revised form 14 September 2010